nature neuroscience

Notch controls embryonic Schwann cell differentiation, postnatal myelination and adult plasticity

Ashwin Woodhoo[1], Maria B Duran Alonso[1], Anna Droggiti[1], Mark Turmaine[1], Maurizio D'Antonio[2], David B Parkinson[3], Daniel K Wilton[1], Raya Al-Shawi[4], Paul Simons[4], Jie Shen[5], Francois Guillemot[6], Freddy Radtke[7], Dies Meijer[8], M Laura Feltri[2], Lawrence Wrabetz[2], Rhona Mirsky[1] & Kristján R Jessen[1]

Notch signaling is central to vertebrate development, and analysis of Notch has provided important insights into pathogenetic mechanisms in the CNS and many other tissues. However, surprisingly little is known about the role of Notch in the development and pathology of Schwann cells and peripheral nerves. Using transgenic mice and cell cultures, we found that Notch has complex and extensive regulatory functions in Schwann cells. Notch promoted the generation of Schwann cells from Schwann cell precursors and regulated the size of the Schwann cell pool by controlling proliferation. Notch inhibited myelination, establishing that myelination is subject to negative transcriptional regulation that opposes forward drives such as Krox20. Notably, in the adult, Notch dysregulation resulted in demyelination; this finding identifies a signaling pathway that induces myelin breakdown *in vivo*. These findings are relevant for understanding the molecular mechanisms that control Schwann cell plasticity and underlie nerve pathology, including demyelinating neuropathies and tumorigenesis.

Schwann cells associate with axons in peripheral nerve trunks. They control neuronal survival in the embryo, provide myelin that is essential for normal movement and sensation in the adult, and control regeneration and repair in injured nerves[1–3].

Notch signaling is integral to the development of the main types of glial cell in the CNS, including astrocytes, Müller cells, radial glia and oligodendrocytes[4,5], and Notch dysfunction has been implicated in a range of CNS diseases, including tumorigenesis and neurodegeneration[6,7]. In view of this, it has become important to understand the role of Notch in the development and pathology of Schwann cells, a system in which the involvement of Notch is surprisingly poorly understood.

Here, we describe the role of Notch in the generation and amplification of Schwann cells in embryonic nerves; in myelination in perinatal nerves; and in the dramatic response of Schwann cells to injury in adult nerves.

For these studies we generated several mouse mutants with conditional activation or inactivation of Notch signaling at different stages of the Schwann cell lineage (see **Supplementary Fig. 1** online for the Notch pathway and our strategy). We focused on limb nerves in which the key transitions of the lineage have been unambiguously established (**Supplementary Fig. 2** online)[1]. First, Schwann cell precursors (SCPs), which occupy mouse limb nerves at embryo day (E) 12/13 (E14/15 in the rat), are formed from neural crest cells. Second, immature Schwann cells, which occupy nerves from E15/16 (E17/18 in the rat), are generated. At this stage, axon/Schwann cell numbers are matched by regulation of Schwann cell proliferation and death. Third, immature cells diverge to form myelinating and non-myelinating cells. Before myelination, which starts around birth, axons and promyelin Schwann cells establish a 1:1 relationship from the irregular groups of axons and Schwann cells (Schwann cell families) that characterize embryonic nerves. This process is known as radial sorting[2]. Remarkably, in injured adult nerves, mature Schwann cells can dedifferentiate to a phenotype related to that of the immature Schwann cell[8–10].

We find that in embryonic nerves Notch accelerates the generation of Schwann cells from SCPs and regulates the size of the Schwann cell pool by controlling proliferation, without affecting apoptosis. In perinatal nerves, Notch acts as a brake to delay myelination, without affecting radial sorting. This finding establishes *in vivo* that myelination is subject to negative transcriptional regulation that opposes forward drivers of the process such as the key myelin transcription factor Krox20. Significantly, in adult nerves, Notch dysregulation results in demyelination. This represents, to the best of our knowledge, the first identification of a signaling pathway that induces myelin breakdown *in vivo*. These data establish that Notch regulates every developmental step of the Schwann cell lineage and controls pathological conditions in adult nerves.

RESULTS

Notch signaling and gliogenesis

Notch signaling in Schwann cells has mainly been studied in the context of initial gliogenesis from the neural crest or from crest-like cells[2]. Even

[1]Department of Cell and Developmental Biology, University College London, London, UK. [2]DIBIT, San Raffaele Scientific Institute, Milan, Italy. [3]Peninsula Medical School, Plymouth, UK. [4]Department of Medicine, University College London, London, UK. [5]Center for Neurologic Diseases, Brigham & Women's Hospital, Harvard Medical School, Boston, Massachusetts, USA. [6]National Institute for Medical Research, London, UK. [7]Ludwig Institute for Cancer Research, University of Lausanne, Epalinges, Switzerland. [8]Department of Cell Biology and Genetics, Erasmus MC, Rotterdam, The Netherlands. Correspondence should be addressed to K.R.J. (k.jessen@ucl.ac.uk).

Received 20 January; accepted 30 March; published online 14 June 2009; doi:10.1038/nn.2323

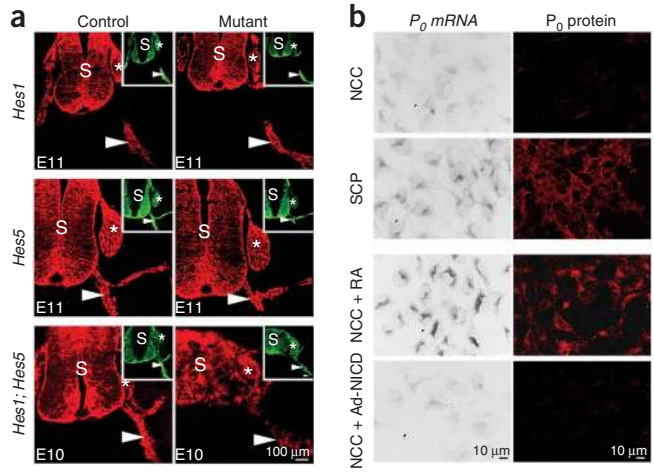

Figure 1 Notch signaling is not involved in the generation of SCPs from neural crest cells. (**a**) Disruption of canonical Notch signaling does not impair gliogenesis in spinal nerves. Both control and mutant embryos express the SCP marker BFABP[1,2] (red) in embryonic nerves (arrowheads) in E11 *Hes1*$^{-/-}$ and *Hes5*$^{-/-}$, and E10 *Hes1*$^{-/-}$*Hes5*$^{-/-}$ mice. The neural tube is disorganized in *Hes1*$^{-/-}$*Hes5*$^{-/-}$ mice[39] but BFABP^{+} cells are still associated with peripheral nerves. Insets: the sections were double immunolabeled with TUJ1 antibodies that bind to class III β-tubulin (green) in axons (arrowheads). DRGs (asterisk) are also BFABP^{+}. S, spinal cord. The percentage of cells (Hoechst^{+} nuclei) in ventral roots or spinal nerves that express BFABP was not statistically different between control and mutant embryos (quantification: **Supplementary Table 1**). (**b**) Notch activation in rat neural crest cells (NCCs) does not upregulate the SCP marker P_0. NCCs (1 d after emigration from neural tube) do not express P_0 mRNA or protein, whereas freshly isolated SCPs express both. Culture of NCCs in retinoic acid (100 ng ml^{-1}) for 3 d (NCC + RA) upregulates P_0 mRNA and protein, reflecting *in vitro* gliogenesis. Notch activation in NCCs, by adenoviral infection (NCC + Ad-NICD), does not upregulate P_0 mRNA or protein after 3 d.

here, the role of Notch remains unclear, as Notch activation in cultured crest cells promotes glial differentiation in rat[11], but not chick[12], whereas Notch activation in the neural crest *in ovo* fails to promote the generation of Schwann cells[13].

When we examined spinal nerves in mouse embryos lacking Hes 1 and/or Hes 5, the effectors of canonical Notch signaling[14], we found no significant effect on SCP formation (**Fig. 1a** and **Supplementary Table 1** online). Consistent with this, Schwann cell generation is reported to occur in mice with neural crest-selective ablation of RBPJ[15], the key transcriptional mediator of canonical Notch signaling[14], although the development of satellite cells and ganglia is impaired.

In vitro, we failed to induce expression of the early glial (SCP) marker protein zero (P_0) by infecting crest cells with an adenovirus expressing NICD, the active intracellular portion of the Notch receptor[14] (Ad-NICD). In parallel experiments, P_0 was readily induced by the gliogenic signal retinoic acid (**Fig. 1b**). These experiments indicate that the first step in the generation of Schwann cells, namely the appearance of SCPs, does not depend on canonical Notch signals.

Notch pathway components in the Schwann cell lineage

To determine the potential importance of the Notch pathway in the rest of the Schwann cell lineage, we showed that its components are expressed in rat sciatic nerves at different ages (**Fig. 2a,b**). Immunolabeling of teased nerves and freshly dissociated cells confirmed that the Notch ligand Jagged 1 was expressed by axons and glia, whereas Notch 1 was detected only on glial cells (**Fig. 2c**).

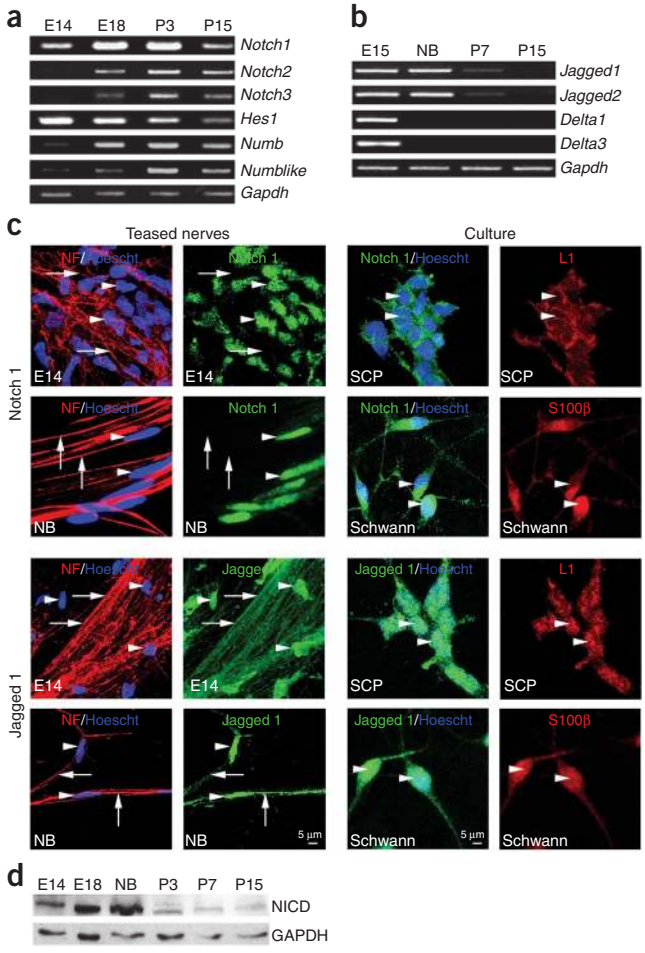

Figure 2 Notch signaling pathway molecules are expressed at different stages in the Schwann cell lineage. (**a**) PCR of Notch pathway components in rat sciatic nerves at E14 (SCPs), E18 (immature Schwann cells) and P3–15 (active myelination). *Notch 1* mRNA increases between E14 and E18/P3, and decreases afterwards. *Notch 2* and *Notch 3* mRNA is not detectable at E14 but found from E18 onwards. *Hes1* is high at E14 and at E18 but lower postnatally. *Numb* and *Numblike* mRNAs are low at E14 but detectable from E18 onwards. *Gapdh*: loading control. (**b**) PCR of Notch ligands in rat DRGs. *Delta 1* and *3* are expressed only at E15, whereas *Jagged 1* and *2* are expressed at E15 and birth but decrease thereafter. *Gapdh*: loading control. (**c**) Expression of Notch 1 and Jagged 1 in E14 and at birth (NB) teased sciatic nerves, and in SCP and Schwann cell cultures. Notch 1 (green) is expressed by SCP and Schwann cells (arrowheads) but is absent from axons in teased nerves (arrows), identified by neurofilament (NF; red). Jagged 1 (green) is seen on axons (arrows) and by SCP and Schwann cells (arrowheads). L1 and S100β were used to identify SCP and Schwann cells, respectively, in dissociated cultures. (**d**) Western blot of NICD in rat sciatic nerve extracts. NICD increases between E14 and E18/NB, and decreases from P3 onwards. GAPDH: loading control.

Notch receptors in developing Schwann cells could therefore be activated by Notch ligands on axons or on the glial cells themselves. The finding that these nerves contain high levels of NICD (**Fig. 2d**) is also consistent with active Notch signaling in embryonic and early postnatal nerves.

Notch drives differentiation of Schwann cell precursors

We next investigated whether Notch controlled the differentiation of SCPs to Schwann cells by examining three changes that mark this

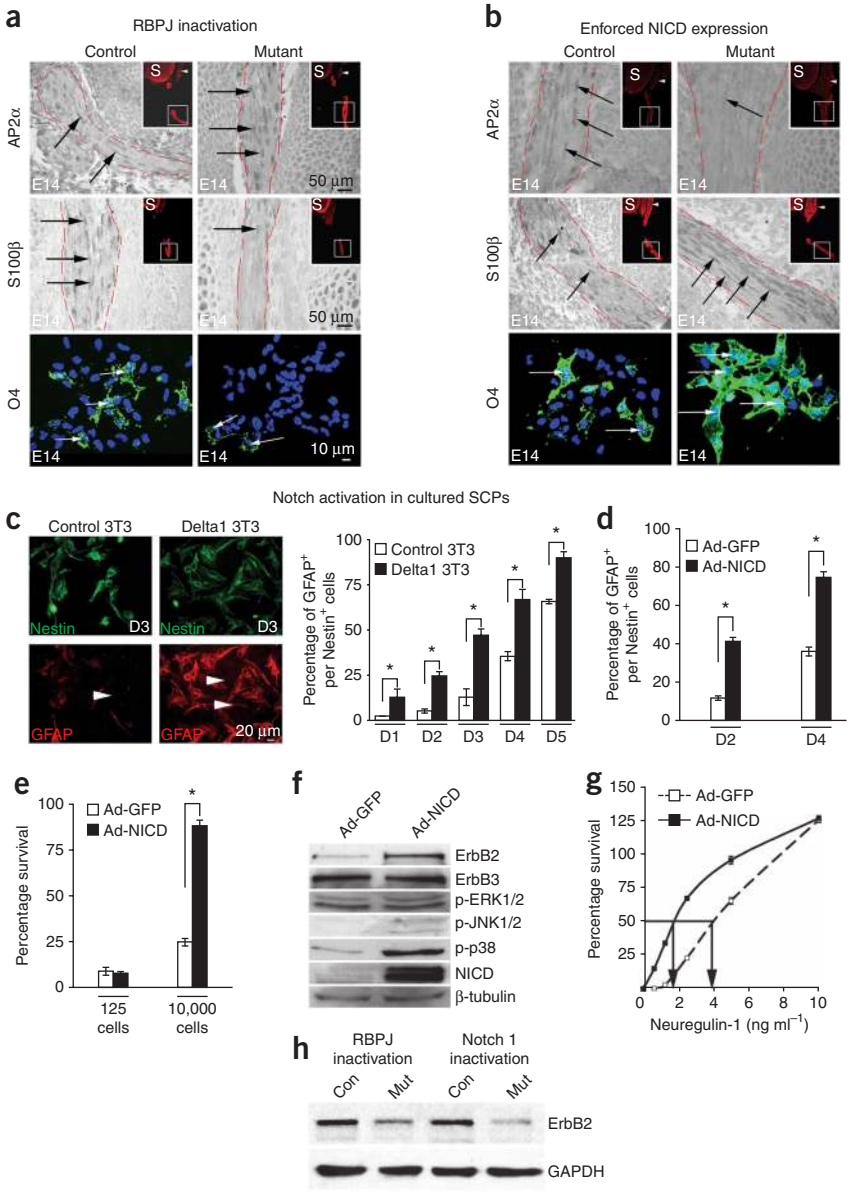

Figure 3 Notch drives Schwann cell generation from SCPs. (**a**,**b**) Top and middle panels, longitudinal sections of E14 hind limb nerves immunolabeled for TUJ1 (inset; red), AP2α or S100β (DAB). Insets, spinal cord (S), DRG (arrowheads). Bottem panels, dissociated cells from E14 sciatic nerves; O4 immunolabeling. Nuclei (blue): Hoechst dye. In *Dhh–cre*$^{+}$*RBPJ*$^{f/f}$ nerves (mutant), AP2α labeling is increased, while S100β and O4 are decreased (**a**). In *Dhh–cre*$^{+}$*CALSL–NICD* nerves (mutant), AP2α labeling is reduced while S100 and O4 are increased (**b**) (quantification: **Supplementary Table 2**). (**c**) Notch activation in SCPs, by co-culture with Delta1-expressing 3T3 cells, accelerates their differentiation into Schwann cells, judged by GFAP expression (red) over a 5-d (D1–5) period. SCPs were 94–99% pure (L1 labeling)[1,2]. Nestin (green) labels SCPs and Schwann cells. (**d**,**e**) Infection of SCPs with Ad-NICD accelerates differentiation into Schwann cells, judged by GFAP expression, 2 (D2) and 4 (D4) d after infection (**d**), and appearance of autocrine survival mechanisms at 2 d in cells plated at high density (10,000 cells; **e**). (**f**) Western blot showing that ErbB2 receptors are elevated in Ad-NICD-infected SCP cultures. Phospho-p38 levels are also elevated. (**g**) The NRG1 concentration needed for 50% survival of Ad-NICD-infected SCPs is only about half that needed for control Ad-GFP-infected cells. (**h**) Western blot showing reduced ErbB2 in mutant (Mut) E14 sciatic nerves from *Dhh-cre*$^{+}$*RBPJ*$^{f/f}$ and *Dhh-cre*$^{+}$*Notch1*$^{f/f}$ mice. Data: mean ± s.e.m., $n = 3$, $^{*}P < 0.01$.

transition: downregulation of the transcription factor AP2α, upregulation of S100β protein and upregulation of the lipid antigen O4[1,2], using loss-of-function and gain-of-function experiments *in vivo*.

Using *Dhh-cre*$^{+}$ mice (**Supplementary Figs. 1** and **2**), we found that Notch inactivation in SCPs, by conditional deletion of *RBPJ*, delayed both AP2α downregulation and S100β upregulation. This was evident from the intensity of immunolabeling and the number of labeled cells in nerve sections (24% increase in AP2α^{+} cells and 30% decrease in S100β^{+} cells). We saw a similar delay (40%) in O4 appearance when E14 nerves were dissociated and immunolabeled (**Fig. 3a**). Similar results were obtained when *Notch 1* was deleted in SCPs (**Supplementary Table 2** online). This indicates that, in normal nerves, canonical (RBPJ-dependent) Notch signaling drives Schwann cell generation.

To show this directly, we generated a mutant with activated Notch in SCPs by breeding *Dhh-cre*$^{+}$ mice with *CALSL-NICD* mice (**Supplementary Figs. 1** and **2**). We found the opposite effect of that seen after Notch inactivation. Downregulation of AP2α and upregulation of S100β were both accelerated (28% decrease in AP2α^{+} cells and 35% increase in S100β^{+} cells). The number of O4^{+} cells increased by 46% (**Fig. 3b**). Therefore NICD activation in SCPs results in premature Schwann cell generation.

This effect of Notch does not depend on other factors that are selectively present *in vivo*, because we found that Notch activation strongly promoted the transition from SCPs to Schwann cells *in vitro* as judged by two independent criteria, the appearance of the Schwann cell marker GFAP[16] and autocrine survival mechanisms[17] (**Fig. 3c–e**). Thus, canonical Notch signaling drives the second step in the generation of Schwann cells from neural crest cells, namely the transition from SCPs to immature Schwann cells.

Notch elevates erbB2 receptors and responsiveness to NRG1

We have shown previously that the transition from SCPs to immature Schwann cells *in vitro* is also promoted by neuregulin-1 (NRG1)[18]. We therefore sought a link between Notch and NRG1 signaling, as seen in the development of radial glia[4,5]. We found that Notch activation in SCPs selectively upregulated the ErbB2 receptors for NRG1 and increased the sensitivity of SCPs to NRG1. This was measured using an NRG1-dependent SCP survival assay[19] (**Fig. 3f,g**).

These results point towards a mechanism by which Notch promotes Schwann cell generation *in vivo*, namely by maintaining high levels of ErbB2 receptors in SCPs, leading to enhanced NRG1 signaling, which is required for SCP survival and is probably involved in promoting lineage progression[2,19,20]. In support of this idea, we found that inactivation of Notch signaling in SCPs *in vivo* resulted in a sharp fall in ErbB2 protein in E14 nerves (**Fig. 3h**).

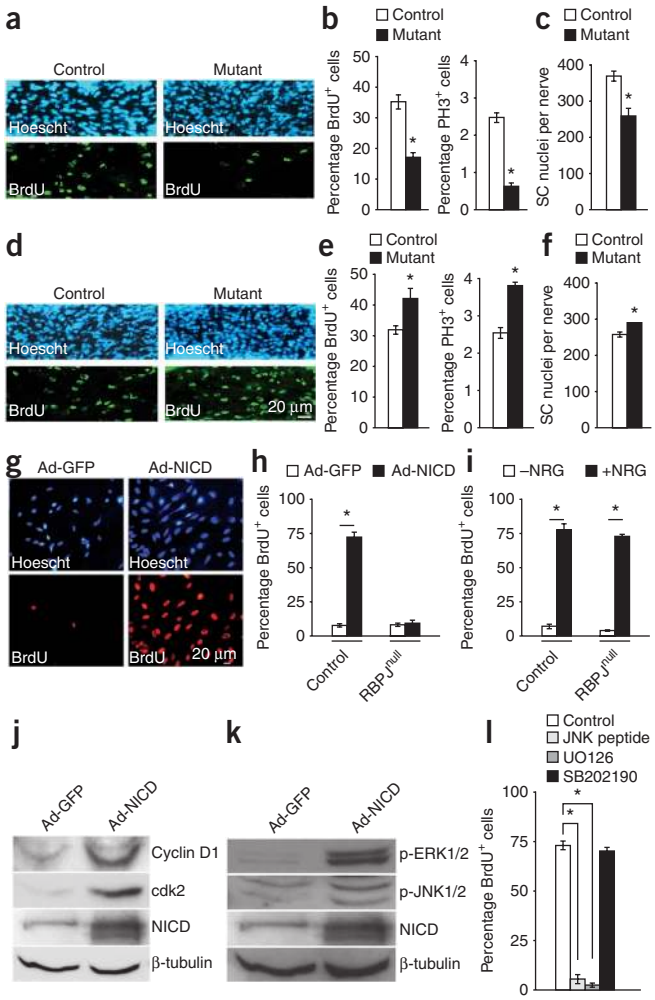

Figure 4 Notch signaling controls the proliferation of immature Schwann cells. (**a**–**c**) RBPJ inactivation. (**a**) E17 nerve sections showing fewer BrdU$^+$ Schwann cells (green) in P_0-*cre*$^+$*RBPJ*$^{f/f}$ nerves. Hoechst (): nuclei. (**b**) RBPJ inactivation significantly reduces BrdU$^+$ and PH3$^+$ cells in E17 nerves. (**c**) The number of Schwann cell (SC) nuclei in P2 nerves is decreased in mutants. (**d**–**f**) Enforced NICD expression. (**d**) E17 nerve sections showing increased BrdU$^+$ Schwann cells (green) in P_0-*cre*$^+$*CALSL-NICD* nerves. (**e**) NICD significantly increases BrdU$^+$ and PH3$^+$ cells in E17 nerves. (**f**) The number of Schwann cell nuclei in P2 nerves is increased in mutants. (**g**-**l**) Notch activation in cultured Schwann cells. (**g**) Ad-NICD-infected Schwann cells have more BrdU$^+$ cells (red) than controls (73.9 ± 2.0 compared to 4.6 ± 1.3). (**h**,**i**) BrdU$^+$ cells in control or RBPJ^{null} Schwann cells after infection with Ad-NICD (**h**), or in the presence of absence of NRG1 (**i**), showing that Ad-NICD, unlike NRG1, fails to induce DNA synthesis in the absence of RBPJ. (**j**,**k**) Western blot shows upregulation of cyclin D1 and cdk2 (**j**) and phospho-ERK 1/2 and phospho-JNK 1/2 (**k**), in Ad-NICD-infected Schwann cells 2 d after infection. NICD demonstrates enforced NICD expression. β-tubulin: loading control. (**l**) Ad-NICD-induced proliferation in Schwann cells *in vitro* is inhibited by JNK peptide (to block JNK phosphorylation) or UO126 (to block ERK1/2 phosphorylation) but not by SB202190 (to block p38 kinase phosphorylation). Data: mean ± s.e.m., $n = 3$, $^*P < 0.01$.

Notch controls Schwann cell proliferation and numbers

Schwann cell generation from SCPs occurs during a period of increasing cell proliferation[2,21,22] that peaks at the immature Schwann cell stage, a time of maximal NICD expression (**Fig. 2d**), indicating that Notch might drive Schwann cell proliferation. When we conditionally deleted *RBPJ* or *Notch 1* using P_0-*cre*$^+$ mice (**Supplementary Figs. 1** and **2**), we found a marked reduction in proliferation (incorporation of 5-bromodeoxyuridine (BrdU) and phosphohistone (PH3) labeling) in both mouse lines (**Fig. 4a–c** and **Supplementary Table 3** online).

To confirm this, we examined proliferation in mice with activated NICD in Schwann cells (P_0-*cre*$^+$ mice bred with *CALSL-NICD* mice; **Supplementary Figs. 1** and **2**). Even though cells in control nerves proliferated rapidly, both BrdU incorporation and PH3 labeling were significantly increased in this mutant (**Fig. 4d**,**e** and **Supplementary Table 3**).

When we counted Schwann cell nuclei in ultra-thin sections of P2 nerves, we found that in all three mutants Schwann cell numbers changed in line with expectations. There was a reduction of 30% and 18% in P_0*cre*$^+$*RBPJ*$^{f/f}$ mice and P_0*cre*$^+$*Notch1*$^{f/f}$ mice, respectively, and an increase of 13% in P_0*cre*$^+$*CALSL-NICD* mice (**Fig. 4c**,**f** and **Supplementary Table 3**). These findings indicate that the canonical Notch pathway is mitogenic for Schwann cells and that NICD elevation is part of the mechanism that controls proliferation and numbers in developing nerves.

To show this directly, we examined proliferation in immunopurified cultured Schwann cells after Notch activation. We found that BrdU incorporation was strongly stimulated by either infection with Ad-NICD (**Fig. 4g**) or co-culture with the immortalized cell line 3T3, expressing the Notch ligand, Delta 1 (data not shown).

To confirm that Notch stimulates proliferation, we used cells that lack RBPJ (*RBPJ*^{null}; *RBPJ*$^{f/f}$ cells treated *in vitro* with Cre adenovirus). Ad-NICD did not induce DNA synthesis in these cells, unlike NRG1 (**Fig. 4h**,**i**). The reduced proliferation observed *in vivo* in mice that lack RBPJ (P_0-*cre*$^+$*RBPJ*$^{f/f}$ mice) therefore reflects reduced Notch, but not NRG1, signaling.

Enforced NICD expression also upregulated the cell cycle markers cyclin D1 and cdk2 (**Fig. 4j**). The mitogenic effect of NICD on Schwann cells involved and depended on phosphorylation of the kinases ERK1/2 and JNK, but not p38 kinase (**Fig. 4k**,**l**). Apoptotic cell death[2,23] (measured by TdT-mediated dUTP nick end (TUNEL) labeling) was unaffected in E17 nerves of the three Notch mutants (**Supplementary Fig. 3** online). In embryonic nerves, therefore, Notch signaling controls Schwann cell proliferation and numbers, but not apoptotic cell death.

Krox20 suppresses Notch signaling in myelinating cells

We next investigated Notch signaling in perinatal nerves during myelination. This process, which starts around birth, is incompatible with proliferation, and most Schwann cells have stopped dividing as they reach the pro-myelin 1:1 stage and start significant myelin gene activation[2,21,24].

Using fluorescence activated cell sorting (FACS) to separate myelinating cells from cells that are not making myelin in P5 nerves, we found that Notch signaling (which drives proliferation) is inactivated in myelinating cells *in vivo* (**Fig. 5a**). This is consistent with the downregulation of NICD protein at the start of myelination in postnatal nerves (**Fig. 2d**).

The transcription factor Krox20 activates myelin genes and suppresses genes associated with immature Schwann cells[1,25–27]. We found that Krox20 suppressed Notch signaling in myelinating cells, as in culture, enforced Krox20 expression by adenoviral infection (Ad-K20) suppressed NICD protein, and *in vivo*, NICD levels remained high in P7 *Krox20*$^{-/-}$ animals, but low in normal nerves (**Fig. 5b**,**c**).

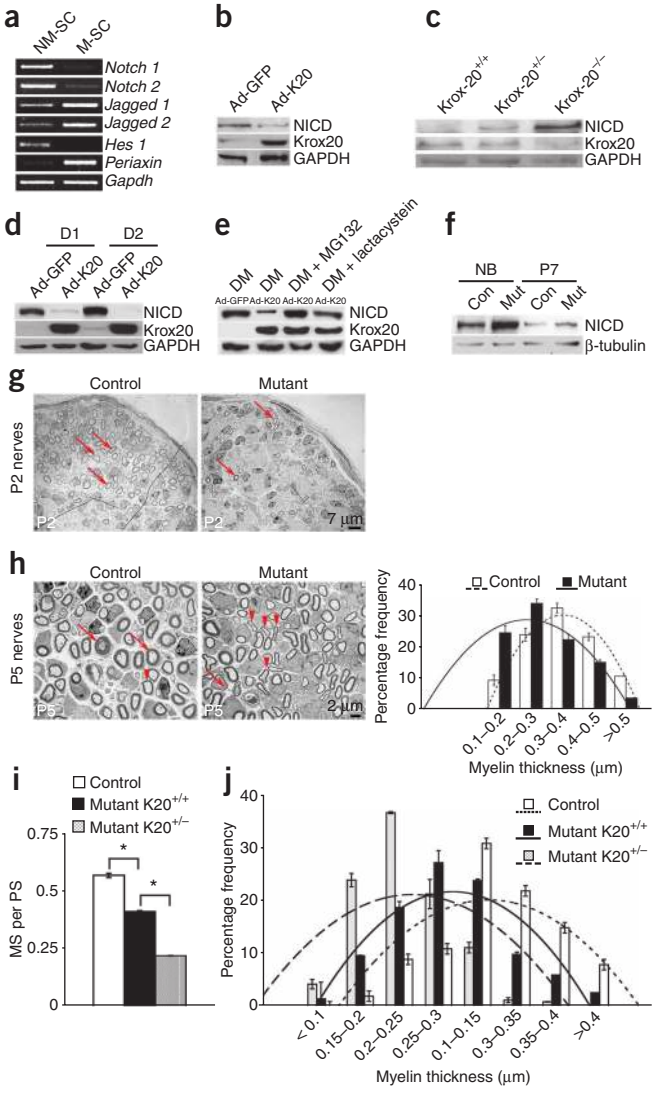

Figure 5 Notch signaling inhibits myelination. (**a**) PCR shows downregulation of *Notch1*, *Notch2* and *Hes1*, and upregulation of *Jagged1* and *Jagged2* in myelinating Schwann cells (M-SC) compared to non-myelinating cells (NM-SC). (**b–f**) Western blots show reduced endogenous NICD after Ad-K20 infection of Schwann cells (**b**), increased endogenous NICD in P7 sciatic nerves from Krox20$^{-/-}$ mice (**c**), reduced exogenous NICD after Ad-K20 infection at 1 (D1) and 2 (D2) d in culture, with exposure to X-ray film too short to reveal endogenous NICD (**d**), abolition of Ad-K20-mediated suppression of NICD expression by the proteosome inhibitors MG132 and lactacystein (**e**), and elevated NICD in *P$_0$-cre$^+$CALSL-NICD* nerves at birth (NB) but not at P7 (**f**). GAPDH/β-tubulin: loading control. (**g**) Enforced NICD expression reduces myelinating Schwann cells (arrows) in mutant nerves (quantification: **Supplementary Table 4**). (**h**) Schwann cells with thin (arrowheads) or thick myelin sheaths (arrows) in P5 nerves with or without enforced NICD expression. Graph depicts the frequency of Schwann cells at different myelin thickness and polynomial trend regression lines. The difference between mutants and controls was significant (quantification: **Supplementary Table 4**). (**i**) Ratio of myelinating to pro-myelinating Schwann cells (MS per PS); (**j**) frequency of Schwann cells at a particular myelin thickness, in control and NICD-overexpressing P2 nerves with normal (Mutant-K20$^{+/+}$) or lower (Mutant-K20$^{+/-}$) Krox20 levels. The mice with reduced Krox20 had significantly reduced myelination (quantification: **Supplementary Table 4**).

Enforced Krox20 expression also suppressed exogenous NICD in Schwann cells (after stable infection with a retrovirus encoding NICD) showing that Krox20 can reduce NICD protein post-translationally (**Fig. 5d**). This depended on the ubiquitin-proteasomal degradation pathway (**Fig. 5e**). As expected, because Krox20 suppresses NICD post-translationally, the enhanced NICD levels in *P$_0$-cre$^+$CALSL-NICD* nerves (**Supplementary Fig. 2**) declined postnatally, when Krox20 was activated upon myelination (**Fig. 5f**).

Notch signaling times the onset of myelination

Because Notch drives proliferation and is downregulated in myelinating cells, we tested whether Notch inhibits myelination. *In vitro*, upregulation of the myelin proteins periaxin and P$_0$ by enforced Krox20 expression was inhibited by simultaneous infection with Ad-NICD (**Supplementary Fig. 4** online). The inhibition was transient, as expected, because Krox20 eventually suppresses exogenous NICD expression (**Fig. 5d**). Enforced NICD expression also blocked cAMP-induced upregulation of myelin proteins[28,29] (**Supplementary Fig. 4**), and myelination in neurone-Schwann cell co-cultures[27] (**Supplementary Fig. 5** online). Notch therefore negatively regulates myelination *in vitro*.

To determine whether Notch is part of the mechanism that times the onset of myelination *in vivo*, we examined nerves from *P$_0$-cre$^+$CALSL-NICD* mice, in which NICD levels are transiently elevated (**Fig. 5f**). We counted the number of myelin sheaths in each nerve profile in P2 nerves, and divided this by the number of Schwann cell nuclei (because NICD affects cell numbers), to obtain a normalized number of myelin sheaths (NNMS). This was reduced from 2.3 in controls to 1.4 in mutants ($n = 10$, $P < 0.01$; **Fig. 5g** and **Supplementary Table 4** online). We measured myelin thickness in P5 nerves, and found that mutant nerves contained significantly more Schwann cells with thin myelin and fewer Schwann cells with thick myelin than controls (**Fig. 5h** and **Supplementary Table 4**). Both measures therefore revealed a significant reduction in myelination in the mutants. P2 mutant nerves also contained less P$_0$ protein (**Supplementary Fig. 5**). Adult mutant nerves, however, had normal g-ratios (axon diameter to fiber diameter), axon diameters and numbers of myelinated axons, reflecting the transient NICD elevation in perinatal nerves (**Supplementary Fig. 6** online).

To confirm that Notch inhibits myelination independently of proliferation, we selectively examined Schwann cells that had already segregated from the Schwann cell families found in developing nerves and formed a 1:1 relationship with axons (pro–myelin cells plus myelinating cells), because proliferation has essentially ceased in these cells[2,21,24]. Within this population, we found a substantial (30%) reduction in the number of myelinating cells, and a corresponding increase in pro-myelin cells (**Supplementary Table 4**). This is the expected outcome if NICD inhibits myelination, that is, the transition of pro-myelin cells to myelinating cells.

We compared this inhibitory effect of NICD in two genetic backgrounds: normal *Krox20$^{+/+}$* and *Krox20$^{+/-}$* mice. Again examining the segregated cells only, we found that the NICD-induced reduction in myelinating cells seen in the normal background (*Krox20$^{+/+}$* mice) was more pronounced in *Krox20$^{+/-}$* mice; myelin sheaths were also substantially thinner (**Fig. 5i,j**). There was no difference in myelination between *Krox20$^{+/+}$* and *Krox20$^{+/-}$* control nerves. Thus, myelination defects in *P$_0$-cre$^+$CALSL-NICD* mice were amplified on a *Krox20$^{+/-}$* background.

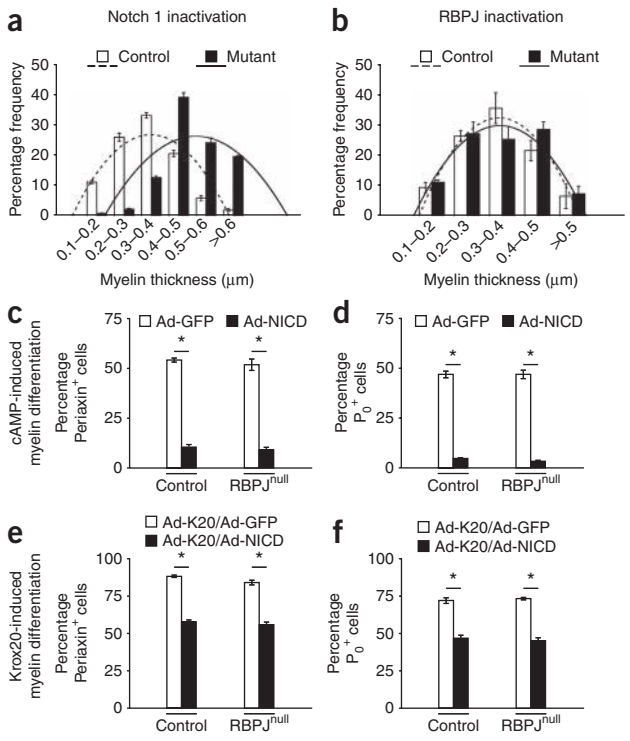

Figure 6 Notch inactivation in Schwann cells leads to RBPJ-independent premature myelination. (**a**) Frequency of Schwann cells with different myelin thickness in P5 sciatic nerves from P_0-*cre*$^+$*Notch1*$^{f/f}$ mice. At each myelin thickness, the difference between mutants and controls was significant (quantification: **Supplementary Table 5**). (**b**) Frequency of Schwann cells at different myelin thickness in P5 sciatic nerves from P_0–*cre*$^+$*RBPJ*$^{f/f}$ mice. At each myelin thickness, the difference between mutants and controls was not significant (quantification: **Supplementary Table 6**). (**c**,**d**) Counts of periaxin$^+$ (**c**) and P_0^+ cells (**d**) show that enforced NICD expression inhibits cAMP-induced myelin protein expression equally in control and RBPJ^{null} Schwann cells. RBPJ^{null} Schwann cells were obtained by treating RBPJ$^{f/f}$ cells with Cre adenovirus *in vitro*. (**e**,**f**) Counts of periaxin$^+$ (**e**) and P_0^+ cells (**f**) show that enforced NICD expression inhibits Krox20-induced myelin protein expression equally in control and RBPJ^{null} Schwann cells. Data: mean ± s.e.m., $n = 3$, $^*P < 0.01$.

Because Notch activation delays myelination, we tested whether, conversely, Notch inactivation *in vivo* would accelerate it. In P_0-*cre*$^+$*Notch1*$^{f/f}$ mice, where Notch 1 has been excised, the myelin sheaths in P5 nerves were significantly thicker than in controls (**Fig. 6a** and **Supplementary Table 5** online). In P2 nerves, there was also a 40% increase in the NNMS. Analysis of segregated cells revealed a striking increase (70%) in the ratio of myelinating cells to pro-myelin cells, confirming that this increase in myelination was independent of proliferation (**Supplementary Table 5**). Thus, myelination is substantially accelerated in Schwann cells that lack Notch 1. These experiments show that Notch is a negative regulator of myelination and Krox20-dependent downregulation of Notch signaling is obligatory for the normal onset of myelination.

Notch controls myelination by RBPJ–independent mechanisms

Although RBPJ is an important downstream effector of Notch, in some cases, an elevation in NICD can signal independently of RBPJ[30,31]. We found that, by any of our measures, P_0-*cre*$^+$*RBPJ*$^{f/f}$ mice had normal myelin, in contrast to that seen in mice without Notch 1 (**Fig. 6b** and **Supplementary Table 6** online). In cultured Schwann cells, Ad-NICD could also suppress cAMP- and Krox20-induced myelin protein expression, even in the absence of RBPJ (**Fig. 6c–f**). Adult nerves from both P_0-*cre*$^+$*Notch1*$^{f/f}$ and P_0-*cre*$^+$*RBPJ*$^{f/f}$ mice were normal (**Supplementary Fig. 6**). Therefore, the negative regulation of myelination by Notch is independent of RBPJ, in contrast to the positive regulation of Schwann cell generation and proliferation, which work through the canonical RBPJ-dependent pathway.

Notch drives Schwann cell demyelination in injured nerves

Remarkably, mature myelinating Schwann cells in adult nerves can dedifferentiate and adopt a phenotype related to that of immature Schwann cells[8–10]. Because Notch acts as a brake to delay myelination, we tested whether Notch was also involved in driving demyelination, a key feature of dedifferentiation. First, we found that infection of P5 Schwann cell cultures with Ad-NICD accelerated the normal loss of myelin *in vitro* (**Fig. 7a**). Second, NICD protein was strongly upregulated in the distal stump of transected nerves 1 and 2 d after they were cut (**Fig. 7b**), a prerequisite for functional involvement of Notch in dedifferentiation. Third, in the absence of *RBPJ* the rate of demyelination in cut sciatic nerves was substantially reduced. The number of intact myelin sheaths was 80% higher and the area occupied by MBP$^+$ myelin 70% greater in nerves lacking *RBPJ* 3 d after transection (**Fig. 7c,d**). Similar results were obtained in mice lacking *Notch 1* (**Supplementary Fig. 7** online).

In the transected facial nerve, the number of cells in the distal stump that retained expression of MBP and the myelin transcription factor Krox20 3 d after transection was also significantly higher in the absence of RBPJ. Furthermore, the number of cells that expressed p75^{NTR}, a marker of immature and non-myelinating cells[1,2], was significantly reduced, indicating delayed reversal to the immature phenotype (**Supplementary Fig. 8** online). These observations show that without canonical RBPJ-dependent Notch signaling, the rate of Schwann cell dedifferentiation in cut nerves is reduced.

To show directly that Notch can accelerate demyelination *in vivo*, we examined myelin disappearance in cut nerves of P_0-*cre*$^+$*CALSL-NICD* mice. First, we confirmed that nerve transection in these mice elevated NICD when compared with cut control nerves (**Fig. 7e**). This was expected because nerve injury will trigger expression of both the endogenous NICD (**Fig. 7b**) and the CALSL-NICD transgene, both of which are suppressed in intact nerves through a Krox-20-dependent mechanism (**Fig. 5e,f**). This increase in NICD resulted in accelerated dedifferentiation. The P_0-*cre*$^+$*CALSL-NICD* nerves contained 50% fewer intact myelinating Schwann cells and the area occupied by MBP$^+$ myelin was 50% smaller than in cut control nerves 3 d after transection (**Fig. 7f,g**). These experiments show that Notch signaling drives demyelination in injured nerves through an RBPJ-dependent mechanism.

Notch initiates demyelination even in uncut nerves

In demyelinating neuropathies, demyelination occurs even though Schwann cells remain in contact with axons until the later stages when axons die[32,33]. The results shown in **Figure 7** raise the question of whether Notch activation is sufficient to trigger demyelination in cells that maintain axonal contact. Initially, we addressed this by showing that infection of established myelinating co-cultures of neurons and Schwann cells with Ad-NICD resulted in myelin damage and apparent breakdown in a high proportion of infected cells, whereas very few Ad-GFP-infected cells had disrupted myelin (**Fig. 8a**).

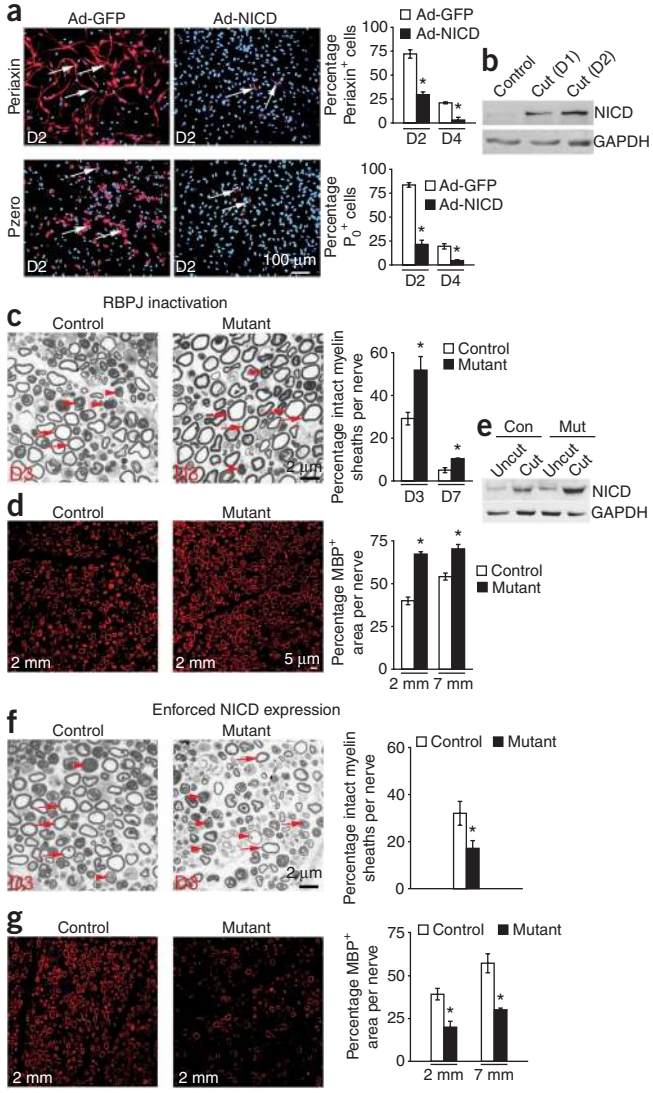

We obtained the same result in adult nerves *in vivo* when we injected intact nerves with Ad-NICD or Ad-GFP. Quantification of demyelination 10 d later showed that Notch activation induced extensive demyelination, revealed by a sixfold increase in the number of degenerating myelin sheaths and 90% loss of MBP$^+$ myelin (**Fig. 8b**,**c**). These results indicate that tight control of Notch signaling is essential for the maintenance of myelin integrity.

Figure 7 Notch promotes demyelination in injured nerves. (**a**) Notch activation accelerates dedifferentiation of P5 myelinating Schwann cells *in vitro*. There are significantly fewer periaxin$^+$ (red) or P_0^+ (red) cells (arrows) in Ad-NICD-infected Schwann cells than in Ad-GFP-infected cultures, 2 (D2) and 4 (D4) d after plating. Nuclei (blue): Hoechst dye. Quantification is shown in right-hand panels. (**b**) Western blot shows elevation of NICD in the distal stump of P60 nerves, 1 (D1) and 2 (D2) d after cut. (**c**,**d**) Schwann cell demyelination is slower in the absence of RBPJ (*P_0-cre$^+$RBPJ$^{f/}$* mice). (**c**) Electron micrographs of the distal stump (2 mm from the cut site) of control and mutant adult nerves, 3 d after cut showing Schwann cells with intact (arrows) or degenerating (arrowheads) myelin profiles. Right, counts at 3 (D3) and 7 (D7) d after cut, 2 mm from cut site ($n = 7$, $^*P < 0.01$). (**d**) MBP immunolabeling of myelin (red) in the distal stump (2 mm from cut site) of control and mutant adult nerves, 3 d after cut. Right, measurement of total MBP$^+$ areas at 2 and 7 mm from cut site ($n = 6$, $^*P < 0.01$). (**e**) Western blot of NICD in uncut and 3 d cut P60 sciatic nerves from *P_0-cre$^+$CALSL-NICD* mice. (**f**,**g**) Schwann cell demyelination is accelerated when NICD is overexpressed (*P_0-cre$^+$CALSL-NICD* mice). For details, see **c** and **d**. Data: mean ± s.e.m., $n = 3$, $^*P < 0.01$.

DISCUSSION

We show that Notch signaling has multiple regulatory functions in Schwann cells that operate right across the lineage, from the SCPs in early embryonic nerves to the control of responses to injury in mature cells. Notch stimulates SCP differentiation and accelerates Schwann cell formation and proliferation in perinatal nerves, inhibits further differentiation and induces dedifferentiation in the adult. On one hand, therefore, the actions of Notch are strikingly pleiotropic and context-dependent. On the other hand, these diverse effects work towards one related biological outcome: the generation of the immature Schwann cell state in development or its closely related counterpart, the denervated Schwann cell in the adult. The role of Notch in the plasticity of postnatal Schwann cells indicates that it might be involved in the numerous Schwann cell disorders that involve dedifferentiation, including tumor formation and demyelinating neuropathies, and raises the possibility that the Notch pathway is relevant for the regeneration of damaged nerves.

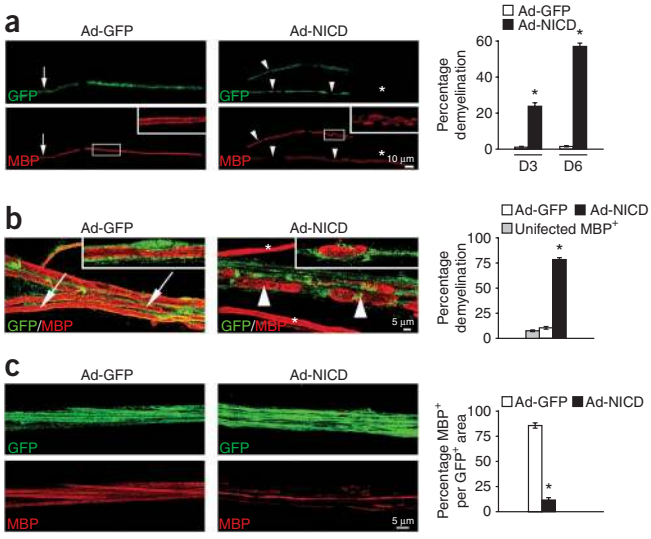

Figure 8 Notch activation induces extensive demyelination *in vitro* and *in vivo*. (**a**) Notch activation results in extensive myelin breakdown in co-cultures of neurons and Schwann cells. After Ad-GFP infection, MBP$^+$ (red) myelin sheaths appear normal at low (arrows) and high magnification (inset). After Ad-NICD infection, many myelin sheaths appear damaged (arrowheads) with ovoids (inset). Non-infected cells have undamaged sheaths (asterisks). Graph, percentage of Ad-GFP$^+$ or Ad-NICD$^+$ cells containing degenerating myelin, 3 (D3) and 6 (D6) d after infection ($n = 6$, $^*P < 0.01$). (**b**,**c**) Notch activation results in extensive myelin breakdown in normal sciatic nerves. (**b**) Higher power view. After Ad-GFP infection, MBP$^+$ myelin sheaths appear normal (arrows). After Ad-NICD infection, many myelin sheaths appear damaged with ovoids (arrowheads). Non-infected cells have undamaged sheaths (asterisks). Graph, percentage of Ad-GFP$^+$ or Ad-NICD$^+$ cells containing degenerating myelin ($n = 10$, $^*P < 0.01$). The low level of myelin degeneration in Ad-GFP$^+$ fibers was similar to that in uninfected MBP$^+$ fibers, indicating that infection with control virus does not induce myelin damage. Insets: single cells with intact (Ad-GFP) or degenerating (Ad-NICD) myelin. (**c**) Lower power view. Most Ad-GFP$^+$ cells contain MBP whereas most Ad-NICD$^+$ cells do not, indicating extensive myelin breakdown. Graph, MBP$^+$ myelin area as a percentage of the total GFP$^+$ area ($n = 10$, $^*P < 0.01$). Data: mean ± s.e.m.

Schwann cell generation

Rather than instructing gliogenesis from the trunk neural crest, we find that Notch signaling acts at the second step of Schwann cell development by promoting the formation of immature Schwann cells from SCPs. SCPs are distinct from migrating neural crest cells because, first, they express glia-associated genes, including P_0, *desert hedgehog* and *BFABP*; second, they differ from crest cells in survival and proliferative responses to extracellular signals; and third, unlike crest cells, they are always in tight apposition to axons, a universal characteristic of glia in the PNS and CNS. Global gene expression analysis also shows that a large group of genes is differentially expressed between SCPs and migratory neural crest cells[1,2]. Using five independent criteria in *in vivo* and culture experiments, we find that Notch inactivation in these cells retards their differentiation into immature Schwann cells whereas Notch activation accelerates it.

Our data can be reconciled with the apparent promotion by Notch of Schwann cell generation from neural crest or crest-like cells, rather than from SCPs, in 14-d assays using the Schwann cell marker GFAP[11,13]. In these experiments, it is plausible that the long period in complex medium allowed some crest cells to generate SCPs. In such cultures, Notch activation would lead to the observed increase in Schwann cells by promoting the transition from SCPs to Schwann cells rather than by acting on neural crest cells, and by stimulating Schwann cell proliferation.

Indirect support for the importance of Notch at this point in development comes from the fact that sensitivity to Notch signaling and Notch expression are much higher at the SCP stage than in migrating crest cells[11]. Thus, we conclude that Notch regulates Schwann cell generation at the SCP–Schwann cell transition.

Schwann cell proliferation

Our data establish canonical Notch signaling as an important positive regulator of Schwann cell proliferation and numbers. The decrease in Schwann cell numbers after Notch inactivation (P_0-*cre*$^{+}$*RBPJ*$^{f/f}$ and P_0-*cre*$^{+}$*Notch1*$^{f/f}$ mice) was mirrored in a quantitatively similar reduction (by 38% and 16% respectively, $P < 0.05$) in the total number of segregated axon–Schwann cell units (pro-myelinating plus myelinating). This relationship between axonal segregation, and therefore the number of cells available for myelination, and total cell numbers has not been demonstrated before to our knowledge.

It follows that the extent of myelination in early nerves is a function of Schwann cell numbers. Notch is, however, unlikely to be involved in the mechanism of segregation itself, because the ratio of segregated cells (pro-myelinating and myelinating) to total cells is not significantly different between Notch-inactivated and control nerves (5.3 ± 0.2 and 5.9 ± 0.3 in P_0-*cre*$^{+}$*RBPJ*$^{f/f}$ mice and controls, respectively, and 6.1 ± 0.3 and 6.0 ± 0.4 in P_0-*cre*$^{+}$*Notch1*$^{f/f}$ mice and controls, respectively). Therefore, the probability of an axon segregating does not vary according to whether Notch signaling is present.

Negative regulation of myelination

Previous experiments have identified a set of positive transcriptional regulators of myelination, namely Krox20, Sox-10, Oct-6 and Brn2, the inactivation of which delay or prevent myelination *in vivo*[1,34]. The present results establish that the transcriptional regulation of myelination during development also incorporates a negative regulatory component. We find that inactivation of Notch 1 promotes *in vivo* myelination and Notch activation delays it. This delay is inversely proportional to levels of the key positive regulator Krox20, indicating that a balance between positive and negative regulatory mechanisms is used to time the onset of myelination. In oligodendrocytes, Notch also negatively regulates myelination *in vitro*[35] and reduced levels of *Notch 1* result in premature myelination *in vivo*[36]. In addition, it has been proposed that Notch activation in oligodendrocyte precursors inhibits their maturation into myelinating oligodendrocytes in multiple sclerosis plaques[37].

We find no enhanced myelination in nerves lacking RBPJ, in contrast to that seen in nerves without Notch1. Experiments on individual cells also show that NICD does not require RBPJ to inhibit the effects of the pro-myelin signals cAMP or Krox20. Together these results reveal an RPBJ-independent signaling pathway that acts as a brake on myelination. Although Notch times two key transitions, from SCPs to immature Schwann cells and immature Schwann cells to myelinating cells, the mechanisms of these two processes are notably different. The first involves RBPJ-dependent promotion of differentiation, whereasthe second involves RBPJ-independent inhibition of differentiation.

Myelin stability and breakdown in cut and normal nerves

After injury to adult nerves, Schwann cells lose their myelin sheaths and dedifferentiate to a phenotype related to that of immature Schwann cells[8–10]. This is accompanied by a sharp increase in NICD. The Notch ligands *Jagged 1* and *2* are also upregulated (A.W., R.M. and K.R.J., unpublished data), but it is not known whether the Schwann cells themselves, macrophages or other cells activate Notch in Schwann cells under these conditions.

In injured nerves, NICD accelerates myelin breakdown. This is severely retarded in the absence of either RBPJ or Notch1 and therefore depends on the canonical RBPJ pathway. The finding that Notch activates different mechanisms to negatively regulate myelination during development and injury was unexpected. It indicates that, more generally, the molecular machinery that controls adult Schwann cell plasticity might differ significantly from the machinery that regulates development.

The present experiments and other recent work indicate that myelin breakdown and other aspects of Schwann cell dedifferentiation are controlled through the activation of a group of transcriptional regulators. In addition to Notch, *in vivo* evidence for this type of function exists for c-Jun[27], and Sox-2, Pax-3 and Id2 might also be involved in Schwann cell dedifferentiation[1,8]. We therefore suggest that Schwann cells contain a set of negative transcriptional regulators that functionally complement the previously established positive regulatory proteins and that myelination and demyelination are determined by a balance between two opposing transcriptional programs[1,8].

The ability of Notch signaling to shift this balance and to drive myelinating cells towards demyelination is shown by the observation that activation of NICD in myelinating cells even of intact, uncut nerves results in severe demyelination. This finding shows that myelin stability and the maintenance of the myelinated state depend crucially on continuous inhibition of Notch signaling. It will be important to determine whether enhanced Notch signaling is a component of the pathogenetic mechanisms in inherited or acquired demyelinating neuropathies. In addition, the fact that Notch is mitogenic in Schwann cells raises the question of whether aberrant Notch activation could lead to the formation of Schwann cell tumors. In support of this idea, Notch can induce transformation in long-term cultured rat Schwann cells that can generate tumors when injected into nude rats[38] and Notch acts as an oncogene in a number of cancers, including brain tumors[6].

METHODS

Methods and any associated references are available in the online version of the paper at http://www.nature.com/natureneuroscience/.

Note: Supplementary information is available on the Nature Neuroscience website.

ACKNOWLEDGMENTS

This work was funded by a Wellcome Trust Programme Grant to K.R.J., R.M. and D.B.P., a Wellcome Trust Project grant to K.R.J. and R.M. and grants from the US National Institutes of Health to M.L.F. and L.W.

AUTHOR CONTRIBUTIONS

A.W. carried out all the experiments with the exception of cAMP myelination assays and PCR analyses, which were performed by M.B.D.A. A.W. was helped by A.D. in *in situ* hybridization experiments, by M.T. in EM sectioning, by M.D. in FACS, by D.B.P. in *in vitro* inhibitor experiments and by D.K.W. in animal husbandry. R.A.-S. and P.S. generated *Hes1*$^{-/-}$*Hes5*$^{-/-}$ cells from frozen embryos. J.S., F.G., F.R., D.M., M.L.F. and L.W. provided the mice. A.W. generated all the figures. A.W., R.M. and K.R.J. designed the experiments. K.R.J., A.W. and R.M. wrote the manuscript.

Published online at http://www.nature.com/natureneuroscience/
Reprints and permissions information is available online at http://npg.nature.com/reprintsandpermissions/

1. Jessen, K.R. & Mirsky, R. The origin and development of glial cells in peripheral nerves. *Nat. Rev. Neurosci.* **6**, 671–682 (2005).
2. Woodhoo, A. & Sommer, L. Development of the Schwann cell lineage: from the neural crest to the myelinated nerve. *Glia* **56**, 1481–1490 (2008).
3. Chen, Z.L., Yu, W.M. & Strickland, S. Peripheral regeneration. *Annu. Rev. Neurosci.* **30**, 209–233 (2007).
4. Louvi, A. & Artavanis-Tsakonas, S. Notch signalling in vertebrate neural development. *Nat. Rev. Neurosci.* **7**, 93–102 (2006).
5. Yoon, K. & Gaiano, N. Notch signaling in the mammalian central nervous system: insights from mouse mutants. *Nat. Neurosci.* **8**, 709–715 (2005).
6. Lasky, J.L. & Wu, H. Notch signaling, brain development and human disease. *Pediatr. Res.* **57**, 104R–109R (2005).
7. Bothwell, M. & Giniger, E. Alzheimer's disease: neurodevelopment converges with neurodegeneration. *Cell* **102**, 271–273 (2000).
8. Jessen, K.R. & Mirsky, R. Negative regulation of myelination: relevance for development, injury and demyelinating disease. *Glia* **56**, 1552–1565 (2008).
9. Scherer, S.S. & Salzer, J.L. Axonal-Schwann cell interactions during peripheral nerve degeneration and regeneration. in *Glial Cell Development: Basic Principles and Clinical Relevance* (eds. Jessen, K.R. & Richardson, W.D.) 299–330 (Oxford, New York, 2001).
10. Müller, H.W. & Stoll, G. Nerve injury and regeneration: basic insights and therapeutic interventions. *Curr. Opin. Neurol.* **11**, 557–562 (1998).
11. Kubu, C.J. *et al.* Developmental changes in Notch1 and numb expression mediated by local cell-cell interactions underlie progressively increasing delta sensitivity in neural crest stem cells. *Dev. Biol.* **244**, 199–214 (2002).
12. Wakamatsu, Y., Maynard, T.M. & Weston, J.A. Fate determination of neural crest cells by NOTCH-mediated lateral inhibition and asymmetrical cell division during gangliogenesis. *Development* **127**, 2811–2821 (2000).
13. Morrison, S.J. *et al.* Transient Notch activation initiates an irreversible switch from neurogenesis to gliogenesis by neural crest stem cells. *Cell* **101**, 499–510 (2000).
14. Bray, S.J. Notch signalling: a simple pathway becomes complex. *Nat. Rev. Mol. Cell Biol.* **7**, 678–689 (2006).
15. Taylor, M.K., Yeager, K. & Morrison, S.J. Physiological Notch signaling promotes gliogenesis in the developing peripheral and central nervous systems. *Development* **134**, 2435–2447 (2007).
16. Jessen, K.R., Morgan, L., Stewart, H.J.S. & Mirsky, R. Three markers of adult non-myelin-forming Schwann cells, 217c (Ran-1), A5E3 and GFAP: development and regulation by neuron–Schwann cell interactions. *Development* **109**, 91–103 (1990).
17. Meier, C., Parmantier, E., Brennan, A., Mirsky, R. & Jessen, K.R. Developing Schwann cells acquire the ability to survive without axons by establishing an autocrine circuit involving insulin-like growth factor, neurotrophin-3 and platelet-derived growth factor-BB. *J. Neurosci.* **19**, 3847–3859 (1999).
18. Brennan, A. *et al.* Endothelins control the timing of Schwann cell generation *in vitro* and *in vivo*. *Dev. Biol.* **227**, 545–557 (2000).
19. Dong, Z. *et al.* Neu differentiation factor is a neuron-glia signal and regulates survival, proliferation and maturation of rat Schwann cell precursors. *Neuron* **15**, 585–596 (1995).
20. Birchmeier, C. & Nave, K.A. Neuregulin-1, a key axonal signal that drives Schwann cell growth and differentiation. *Glia* **56**, 1491–1497 (2008).
21. Stewart, H.J., Morgan, L., Jessen, K.R. & Mirsky, R. Changes in DNA synthesis rate in the Schwann cell lineage in vivo are correlated with the precursor-Schwann cell transition and myelination. *Eur. J. Neurosci.* **5**, 1136–1144 (1993).
22. Yu, W.M., Feltri, M.L., Wrabetz, L., Strickland, S. & Chen, Z.L. Schwann cell–specific ablation of laminin gamma1 causes apoptosis and prevents proliferation. *J. Neurosci.* **25**, 4463–4472 (2005).
23. Winseck, A.K. & Oppenheim, R.W. An in vivo analysis of Schwann cell programmed cell death in embryonic mice: the role of axons, glial growth factor, and the pro-apoptotic gene Bax. *Eur. J. Neurosci.* **24**, 2105–2117 (2006).
24. Webster, H.D., Martin, R. & O'Connell, M.F. The relationships between interphase Schwann cells and axons before myelination: a quantitative electron microscopic study. *Dev. Biol.* **32**, 401–416 (1973).
25. Topilko, P. *et al.* Krox-20 controls myelination in the peripheral nervous system. *Nature* **371**, 796–799 (1994).
26. Parkinson, D.B. *et al.* Regulation of the myelin gene periaxin provides evidence for Krox-20–independent myelin-related signaling in Schwann cells. *Mol. Cell. Neurosci.* **23**, 13–27 (2003).
27. Parkinson, D.B. *et al.* c-Jun is a negative regulator of myelination. *J. Cell Biol.* **181**, 625–637 (2008).
28. Lemke, G. & Chao, M. Axons regulate Schwann cell expression of the major myelin and NGF receptor genes. *Development* **102**, 499–504 (1988).
29. Morgan, L., Jessen, K.R. & Mirsky, R. The effects of cAMP on differentiation of cultured Schwann cells: progression from an early phenotype (04+) to a myelin phenotype (P0+, GFAP−, N-CAM−, NGF receptor−) depends on growth inhibition. *J. Cell Biol.* **112**, 457–467 (1991).
30. Luo, D., Renault, V.M. & Rando, T.A. The regulation of Notch signaling in muscle stem cell activation and postnatal myogenesis. *Semin. Cell Dev. Biol.* **16**, 612–622 (2005).
31. Martinez Arias, A., Zecchini, V. & Brennan, K. CSL-independent Notch signaling: a checkpoint in cell fate decisions during development. *Curr. Opin. Genet. Dev.* **12**, 524–533 (2002).
32. Nave, K.A., Sereda, M.W. & Ehrenreich, H. Mechanisms of disease: inherited demyelinating neuropathies from basic to clinical research. *Nat. Clin. Pract. Neurol.* **3**, 453–464 (2007).
33. Suter, U. & Scherer, S.S. Disease mechanisms in inherited neuropathies. *Nat. Rev. Neurosci.* **4**, 714–726 (2003).
34. Svaren, J. & Meijer, D. The molecular machinery of myelin gene transcription in Schwann cells. *Glia* **56**, 1541–1551 (2008).
35. Wang, S. *et al.* Notch receptor activation inhibits oligodendrocyte differentiation. *Neuron* **21**, 63–75 (1998).
36. Givogri, M.I. *et al.* Central nervous system myelination in mice with deficient expression of Notch1 receptor. *J. Neurosci. Res.* **67**, 309–320 (2002).
37. John, G.R. *et al.* Multiple sclerosis: re-expression of a developmental pathway that restricts oligodendrocyte maturation. *Nat. Med.* **8**, 1115–1121 (2002).
38. Li, Y. *et al.* Notch and Schwann cell transformation. *Oncogene* **23**, 1146–1152 (2004).
39. Hatakeyama, J. *et al.* Hes genes regulate size, shape and histogenesis of the nervous system by control of the timing of neural stem cell differentiation. *Development* **131**, 5539–5550 (2004).

ONLINE METHODS

Animals. We used a cre/lox strategy to inactivate Notch signaling. To delete *RBPJ* in SCPs, mice homozygous for the $RBPJ^{f/f}$ locus[40] were crossed with mice in which Cre expression is controlled by desert hedgehog regulatory sequences and directed to SCPs around E12 ($Dhh\text{-}cre^{+}$ mice)[41]. The $Dhh\text{-}cre^{+}RBPJ^{f/+}$ offspring were backcrossed with $RBPJ^{f/f}$ mice to generate $Dhh\text{-}cre^{+}RBPJ^{f/f}$ (mutants) and $Dhh\text{-}cre^{-}RBPJ^{f/f}$ (controls). To delete *Notch1*, we used mice homozygous for the $Notch1^{f/f}$ locus[42].

For Notch activation in SCPs, we crossed *CALSL-NICD* transgenic mice, in which transcription of an *NICD* transgene is blocked by an upstream floxed 'stop–cassette'[43], with $Dhh\text{-}cre^{+}$ mice to generate $Dhh\text{-}Cre^{+}NICD$ (mutants) and $Dhh\text{-}cre^{-}NICD$ (controls). To activate or inactivate Notch signaling in Schwann cells, the same strategy was used, except that mice in which Cre expression is controlled by the P_0 gene and activated selectively in Schwann cells around E15 ($P_0\text{-}cre^{+}$ mice)[44], were used in place of $Dhh\text{-}cre^{+}$ mice to generate the various mutants. **Supplementary Figure 2** shows cre expression and recombination efficiency in mutants.

Hes 1, *Hes 5* and *Krox20* null mice, and *Hes1Hes5* double null mice have been described[25,39]. Primers for genotyping and recombination experiments are in **Supplementary Table 7** online. Time-mated females, postnatal and adult rats and imprinting control region (ICR) mice were from the Biological Services Unit at UCL.

Electron microscopy and morphometric analyses. Processing of nerves and analyses of morphometry, G–ratios and axon diameters in adults were as described[27,45,46]. For early myelination studies, images of whole P2 and P5 nerves were acquired and analyzed using NIH ImageJ. At P2, the number of myelin sheaths (MS) per nerve profile was counted andeither divided by the number of Schwann cells, identified by their nuclei and association with axons, to obtain the normalized number of myelin sheaths (NNMS), or expressed as a ratio of the number of pro-myelinating Schwann cells (PS; non-myelinating Schwann cells in a 1:1 relationship with an axon) (MS per PS). In P5 nerves, we determined the axon diameter and myelin thickness of about 500 sheaths and calculated the proportion of Schwann cells within defined myelin thickness ranges.

Nerve transection. Nerve transection was performed as described, according to UK Home Office guidelines[27,47]. Distal stumps and the control uninjured contralateral nerves were processed for western blotting, immunohistochemistry (IHC) or electron microscopy (EM) analysis, or dissociated and plated on coverslips for immunolabeling. For EM analysis, images of the whole nerve were acquired and the number of intact myelin sheaths counted and expressed as a percentage of the total number of myelinating Schwann cells in the uninjured contralateral nerve. For IHC, paraffin sections were immunolabeled for MBP and confocal pictures of the whole nerve acquired. The MBP^{+} myelin area was calculated and expressed as a percentage of MBP^{+} myelin in the uninjured contralateral nerve using NIH ImageJ.

***In vivo* adenoviral infections.** We exposed sciatic nerves of anaesthetized P60 ICR mice and injected 1 µl of Ad-NICD or Ad-GFP (10^{12} virions ml^{-1}) into the endoneurium (ten animals per group). The nerves were dissected out 10 d later, teased onto microscope slides and immunolabeled for MBP. Confocal pictures of the infected Schwann cells (GFP expression) and myelin (MBP expression) were acquired and analyzed. To determine the extent of Notch–induced myelin breakdown, we counted the number of GFP^{+} Schwann cells with damaged myelin profiles. We also determined the area of MBP^{+} myelin occupied by GFP^{+} cells using NIH Image J.

Neural crest cell cultures. Neural tubes from E11 rat embryos were dissected out and plated on a PDL-fibronectin coated 35-mm Petri dish containing 2 ml of defined medium (DM) (1:1 mixture of DMEM and Ham's F12, supplemented with transferrin (100 µg ml^{-1}), progesterone (60 ng ml^{-1}), putrescine (16 µg ml^{-1}), thyroxine (0.4 µg ml^{-1}), tri-iodothyronine (10.1 ng ml^{-1}), dexamethasone (38 ng ml^{-1}), selenium (160 ng ml^{-1}), BSA (0.3 mg ml^{-1}), penicillin (100 IU ml^{-1}), streptomycin (100 IU ml^{-1}) and glutamine (2 mM)) supplemented with NRG1 (10 ng ml^{-1}), IGF1 (100 ng ml^{-1}), N-acetyl cysteine (1 mM), FGF2 (3 ng ml^{-1}) and insulin (10^{-9} M). Explants were cultured for 24 h at 37 °C and 5% CO_2 after which the neural tubes were excised with a needle using an inverted microscope, leaving the neural crest cells attached to the dish. The cells were then dissociated by incubating for 3 min in 200 µl versene (0.2 mg ml^{-1} EDTA, 0.01% PBS, 0.005% Phenol Red in ultra pure deionized water) containing three drops of enzyme cocktail (collagenase (2 mg ml^{-1}), hyaluronidase (1.2 mg ml^{-1}) and trypsin inhibitor (0.3 mg ml^{-1}) in DMEM). After centrifugation the cells were resuspended in the relevant medium and plated.

Schwann cell precursor cultures. We dissected sciatic nerves from E14 rat embryos and incubated them for 1 h in enzyme cocktail at 37 °C. The cell suspension was centrifuged and resuspended in DM supplemented with NRG1 (10 ng ml^{-1}) and insulin (10^{-9} M).

Serum-purified Schwann cell cultures. Sciatic nerves were dissected from newborn or postnatal day 3 (P3) rats and dissociated by digestion in 0.25% trypsin, 0.4% collagenase in DMEM at 37 °C and 5%CO2 and 95% air for 35 min with trituration at the end. The cell suspension was then centrifuged and cultured for 3 d in DMEM containing 10% FCS (FCS) and cytosine arabisnoside (AraC) (10^{-3} M), which kills contaminating fibroblasts. After 3 d in culture, more than 95% of the cells are Schwann cells.

Neuron/Schwann cell co-cultures. We prepared co-cultures of neurons and myelinating Schwann cells by adding together purified E15 rat DRG neurons and purified neonatal Schwann cells[27] stably infected with an NICD-expressing retrovirus. Myelination was induced by adding 50 mg ml^{-1} ascorbic acid to the medium, which contained DM, 10% FCS and NGF (50 ng ml^{-1}). We used P_0 antibodies to immunolabel myelin segments.

For demyelination assays, organotypic DRG/SC co-cultures were set up and myelination induced with ascorbic acid over two weeks. Thereafter, the cultures were infected with Ad-GFP or Ad-NICD adenovirus. At 3 and 6 d after infection, the cultures were fixed and immunolabeled with MBP antibodies. The number of GFP^{+} cells with damaged myelin profiles was counted and expressed as a percentage of the total number of myelin segments.

Viral constructs. Adenoviral constructs expressing GFP/Krox20 (Ad-K20) and its matched GFP control (Ad-GFP) were a gift from J. Milbrandt (Washington University, St. Louis, Missouri)[26,27]. Adenoviral constructs expressing GFP/NICD (Ad-NICD) and its matched GFP control (Ad-GFP) were a gift from G.P. Dotto (University of Lausanne, Epaninges, Switzerland)[48]. The cDNAs for NICD, obtained by PCR from the full-length human Notch1 cDNA (amino acids 1760–2566) and the cDNAs for mouse full length Delta 1 (amino acids 14–2190) were cloned into the retroviral plasmid vector pBABEpuro, and the GP+E ectotropic packaging cell line was then stably transfected with the plasmid DNA. We used plasmids without the transgene as a control vector. Retroviral supernatant obtained from the infected GP+E cells was used to infect confluent cells, followed by puromycin (1 mg ml^{-1}) selection.

Inhibitors. Specific inhibitors used were: UO126 (ERK 1/2 phosphorylation inhibitor; 10 mM, Calbiochem), SB202190 (p38 phosphorylation inhibitor; 10 mM, Calbiochem), JNK peptide (JNK 1/2 phosphorylation inhibitor; 10 mM, a gift from H. Mehmet (Imperial College, London, UK[27])), MG132 (10 mM, Calbiochem) and lactacystein (10 mM, Calbiochem).

cAMP myelination assay. A cAMP analog, dibutryl cAMP (10^{-3} M), was added to cultures, as mentioned in the text. The cells were then fixed after 1 d for Krox20 ICC, 2 d for periaxin ICC or 3 d for P_0 ICC[26,27].

Fluorescence-activated cell sorting (FACS). We separated immunopanned P5 Schwann cells into myelinating and non-myelinating populations by FACS[47]. Schwann cells were isolated from 10 P5 rat pups, purified by immunopanning with OX-7 antibodies, immunolabeled with antibodies against GalC, which at this age is expressed by myelinating Schwann cells but not by non-myelinating Schwann cells[49], and then sorted using a Becton-Dickinson FACSCalibur machine (BD), which first sorted the live cells from the dead cells and then separated the fluorescent ($GalC^{+}$) from the non-fluorescent cells ($GalC^{-}$). The two populations were collected and the mRNA extracted and processed for RT-PCR.

doi:10.1038/nn.2323

Immunohistochemistry (IHC) and immunocytochemistry (ICC). For frozen sections, samples were fixed for 4 h in 4% PFA, placed in 30% sucrose overnight, frozen in OCT and sectioned (10 μm) using a cryostat. For paraffin sections, samples were fixed in PFA in PBS at 4 °C overnight, dehydrated and embedded in paraffin wax. Paraffin sections (5 μm) were rehydrated and subjected to antigen retrieval in 10 mM sodium citrate buffer (pH 6.0). For teased nerves, nerves were dissected out, immediately fixed in 4% PFA in PBS for 10 min, teased on microscope slides and allowed to dry.

The samples were incubated in 0.2% triton in blocking solution (BS: PBS containing 10% FCS, 0.1% lysine and 0.02% sodium azide) followed by overnight incubation at 4 °C with the following primary antibodies: BFABP (rabbit, 1:5000); TUJ1 (mouse, 1:5000, Covance); S100β (rabbit, 1:1000, Dakopatts); AP2α (rabbit, 1:1000; Santa Cruz Biotechnology); MBP (mouse, 1:500, Sternberger Monoclonals); Jagged 1 (rabbit, 1:200, Santa Cruz Biotechnology); Notch 1 (hamster, 1:100, Upstate); and neurofilament (mouse, 1:50). For S100β and AP2α IHC, HRP-conjugated secondary antibodies were used followed by HRP substrate, diaminobenzidine. For other IHC, secondary antibodies for detection of rabbit or mouse antibodies were labeled by fluorescence (FITC or Cy3; Cappel MP biomedicals or Jackson Immunoresearch Labs).

For GFAP and nestin ICC, cultures were fixed with 4% PFA in PBS for 10 min, permeabilized with methanol (−20 °C) for 10 min and the following primary antibodies applied overnight at 4 °C: GFAP (rabbit, 1:200, Dakopatts); nestin (mouse, 1:2000, Developmental Studies Hybridoma Bank). Krox20, periaxin and P_0 ICC procedures were as described[26,27]. For O4 antigen/L1 ICC or $p75^{NTR}$ ICC, unfixed cells were incubated with O4 hybridoma supernatant (mouse, 1:1), and L1 hybridoma supernatant (rat, 1:1) or $p75^{NTR}$ antibody (rabbit, 1:200, Cell Signaling Technology) diluted in MEM-Hepes/10% FCS for 1 h, followed by application of appropriate secondary antibodies and post-fixation with 4% PFA in PBS for 5 min.

Apoptotic cells were detected by TUNEL labeling. Proliferative cells were detected *in vivo* in E17 sciatic nerves by BrdU incorporation and immunolabeling or PH3 immunolabeling and *in vitro* were detected by BrdU incorporation[46]. *P_0 in situ* hybridization has been described[50].

Western Blotting. Protein extracts were prepared and blotted as described[26,27]. The following antibodies were used: β-tubulin (mouse, 1:2000, Sigma), Cdk 2 (rabbit, 1:500, Santa Cruz Biotechnology), Cyclin D1 (mouse, 1:500, Santa Cruz Biotechnology), ErbB2 (rabbit, 1:500, Santa Cruz Biotechnology), ErbB3 (rabbit, 1:500, Santa Cruz Biotechnology), GAPDH (mouse, 1:5000 Abcam), Krox20 (rabbit, 1:2500, Covance), NICD (mouse, 1:1000, Chemicon), phospho-ERK 1/2 (mouse, 1:2000, Sigma), phospho-JNK 1/2 (rabbit, 1:1000, Cell Signaling Technology), phospho-p38 (rabbit, 1:1000, Cell Signaling Technology), P_0 (mouse, 1:2000, Astexx). HRP-conjugated secondary antibodies were used and developed with ECL reagent (Amersham Biosciences). Experiments were repeated three times with fresh samples and representative pictures are shown. For *in vitro* experiments, fresh cultures were used each time. For *in vivo* experiments, embryonic nerves were isolated from several embryos from at least two litters and postnatal nerves from at least two animals were used. Uncropped pictures of western blots are in **Supplementary Figure 9** online.

Semi-quantitative PCR. Protocols for RNA extraction from nerve samples and cDNA synthesis have been described[47] and the primers used are found in **Supplementary Table 7**. Experiments were repeated three times with fresh samples and representative pictures are shown. For each experiment, embryonic nerves or DRGs were isolated from several embryos. For isolation of postnatal nerves, at least two animals were used.

Statistical analysis. All values are shown as mean ± s.e.m. from at least three independent experiments and considered significant if $P < 0.01$. Significance between groups was calculated using Student's *t*-tests.

40. Tanigaki, K. *et al.* Notch-RBP-J signaling is involved in cell fate determination of marginal zone B cells. *Nat. Immunol.* **3**, 443–450 (2002).
41. Jaegle, M. *et al.* The POU proteins Brn-2 and Oct-6 share important functions in Schwann cell development. *Genes Dev.* **17**, 1380–1391 (2003).
42. Radtke, F. *et al.* Deficient T cell fate specification in mice with an induced inactivation of Notch1. *Immunity* **10**, 547–558 (1999).
43. Yang, X. *et al.* Notch activation induces apoptosis in neural progenitor cells through a p53-dependent pathway. *Dev. Biol.* **269**, 81–94 (2004).
44. Feltri, M.L. *et al.* P0-Cre transgenic mice for inactivation of adhesion molecules in Schwann cells. *Ann. NY Acad. Sci.* **883**, 116–123 (1999).
45. Sharghi-Namini, S. *et al.* The structural and functional integrity of peripheral nerves depends on the glial-derived signal desert hedgehog. *J. Neurosci.* **26**, 6364–6376 (2006).
46. D'Antonio, M. *et al.* TGFbeta type II receptor signaling controls Schwann cell death and proliferation in developing nerves. *J. Neurosci.* **26**, 8417–8427 (2006).
47. D'Antonio, M. *et al.* Gene profiling and bioinformatic analysis of Schwann cell embryonic development and myelination. *Glia* **53**, 501–515 (2006).
48. Rangarajan, A. *et al.* Notch signaling is a direct determinant of keratinocyte growth arrest and entry into differentiation. *EMBO J.* **20**, 3427–3436 (2001).
49. Jessen, K.R., Morgan, L., Brammer, M. & Mirsky, R. Galactocerebroside is expressed by non-myelin-forming Schwann cells *in situ*. *J. Cell Biol.* **101**, 1135–1143 (1985).
50. Morgan, L., Jessen, K.R. & Mirsky, R. Negative regulation of the P0 gene in Schwann cells: suppression of P0 mRNA and protein induction in cultured Schwann cells by FGF2 and TGF beta 1, TGF beta 2 and TGF beta 3. *Development* **120**, 1399–1409 (1994).